Numerical study on modelling perforated elements using porous baffle interface and porous region

Giada Kyaw Oo D'Amore
Department of Engineering and Architecture, University of Trieste, Trieste, Italy, and

Francesco Mauro
NAOME, University of Strathclyde, Glasgow, UK

Accepted 10 October 2021

Abstract

Purpose – This study aims to analyze simplified methods for modelling the flow through perforated elements (i.e. porous baffle interface and porous region), searching for a faster and easier way to simulate these components. The numerical simulations refer to a muffler geometry available in literature as a case study.

Design/methodology/approach – The installation of scrubber onboard ships to satisfy the International Maritime Organization emissions regulations is a reliable and efficient solution. However, scrubbers have considerable dimensions, interfering with other exhaust line components. Therefore, scrubber installation in the funnels requires integration with other elements, for example, silencers. Perforated pipes and plates represent the main elements of scrubber and silencers. The study of their layout is, therefore, necessary to reduce emissions and noise. Numerical simulations allow evaluating the efficiency of integrated components.

Findings – The study highlights that velocity and pressure predicted by the simplified models have a strong correlation with the resistance coefficients. Even though the simplified models do not accurately reproduce the flow through the holes, the use of such models allows a fast and easy comparison between concurrent muffler geometries, giving aid in the early design phases.

Originality/value – The lack of general guidelines and comparisons in the literature between different modelling strategies of perforated elements supports the novelty of the present work and its impact on design applications. Study the flow inside scrubbers and mufflers is fundamental to evaluate their performances. Therefore, having a simple numerical method is suited for industrial applications during the design process.

Keywords CFD simulations, Perforated pipe, Porous region, Porous baffle interface, Marine silencer

Paper type Research paper

1. Introduction

During the past few years, the global climate changes and the environmental problems related to the extensive use of fossil fuels lead to an increasing interest in alternative energy production systems (Neshat *et al.*, 2019). Also, in the maritime sector, with the rapid development of the global shipping industry, the IMO (International Maritime Organization) has restricted the limits imposed by MARPOL (Marine Pollution) 73/78 Annex VI (IMO, 2008) on ships' emissions, especially considering SO_x (sulphur oxides) and NO_x (nitrous

Funding: No funding was received for conducting this study.
Conflicts of interest: The authors have no conflicts of interest to declare that are relevant to the content of this article.

oxides). Nowadays, selective catalytic reduction (SCR) systems are the most effective technology for marine NO_x emissions control (Chen and Lv, 2015). The following strategies are the most effective to reduce SO_x emissions (Johnsen *et al.*, 2019): fuels with low sulphur content (e.g. marine gas oil), alternative fuels (e.g. liquefied natural gas) or alternative propulsion systems (e.g. fuel cell). However, the mentioned solutions present disadvantages for costs and operating limits (Johnsen *et al.*, 2019; Mungodla *et al.*, 2019). Moreover, the adoption of such systems onboard ships already in navigation leads to the necessity of refitting the entire propulsion system. A scrubber represents an alternative solution granting an emission abetment system compliant with SO_x regulation even using traditional fuels (e.g. heavy fuel oil) with a high sulphur content and low cost (Johnsen *et al.*, 2019).

Therefore, the onboard installation of both SCR and scrubber systems represents a reliable solution to satisfy NO_x and SO_x emissions limits, especially for existing vessels. The scrubber installation does not present operational limits for ships, does not require the propulsion system refitting, has a lower cost per ton of SO_x emissions reduced and has a lower climate impact in terms of CO_2 (carbon dioxide) emitted (Fan *et al.*, 2020). However, considering the vast size of the exhaust line components and the limitation of spaces onboard, integrate systems such as SCR and scrubber with, for example, the silencer becomes mandatory to mount the scrubbers in the funnels (Chen and Lv, 2015).

All these components contain perforated pipes or perforated plates. These elements optimize the chemical reactions breaking down the SO_x and NO_x and the acoustic performances (Chen and Lv, 2015; Selvakumar and Kim, 2016; Suganeswaran *et al.*, 2014). The design process of SCRs, scrubbers and silencers may use both CFD (computational fluid dynamics) and finite element method analysis (Fu *et al.*, 2021). However, CFD allows evaluating flow pressure and velocity and chemical reactions effectiveness (Chen and Lv, 2015; Selvakumar and Kim, 2016; Zhang *et al.*, 2018), being the most suitable approach to study mufflers (Venkatagiri *et al.*, 2020). The proper simulation of the flow field is a particularly important aspect for mufflers designs as allows to calculate the acoustic properties of the system in presence of flow and to evaluate the backpressure generated by the muffler itself (Liu *et al.*, 2020; Shinde *et al.*, 2020). In fact, the higher is the backpressure, the lower is engine efficiency of engine (Thirumurugaveerakumar, 2020).

The advantages of a faster and simpler model to simulate perforated elements are underlined by the widespread study and optimization of mufflers (Barua and Chatterjee, 2019; Liu *et al.*, 2019; Narasimhan *et al.*, 2020; Liu et *al.*, 2021) and the importance of perforated elements (Jun *et al.*, 2018; Mishra *et al.*, 2018; Swamy *et al.*, 2020; Kashikar *et al.*, 2021;) for the determination of acoustic properties and backpressure. In fact, for mufflers, the cross-flow perforated pipes/plates are the most significant acoustic noise reduction elements and the most critical ones for backpressure (Fu *et al.*, 2016; Narasimhan *et al.*, 2020; Wang *et al.*, 2013; Venkatagiri *et al.*, 2020).

Analyzing the available literature, except for few studies investigating the acoustic properties of perforated elements with simplified geometries that do not model the holes (e.g. considering the impedance (Li *et al.*, 2018) or the Rayleigh conductivity (Mendez and Eldredge, 2009), there is the lack of papers reporting general guidelines and comparisons between different CFD modelling strategies (e.g. porous baffle interface or porous region), giving evidence of such modeling also on the pressure drop. Some cases are available for heat exchangers, where the tubes bundles are modeled with a porous model that introduces volume porosity, surface permeability and a distributed flow resistance as parameters (Yang *et al.*, 2014; Prithiviraj and Andrews, 1998), comparing obtained results with complete geometry ones.

Considering perforated elements in mufflers, the holes diameter and the porosity are the principal characterizing parameters (Rao and Varma, 2007; Chen *et al.*, 2020). Simplified models can save modelling time during the initial muffler design process, especially for multiple-holes geometries or configurations. In such cases, a porous interface/region neglects the necessity to re-draw and re-mesh the entire geometry. Therefore, the process needs the modification of only some input parameters. However, with the adoption of a porous baffle interface or a porous region, the holes flow is not well captured, as the fluid crosses the pipe through the entire interface/region length. Furthermore, a proper set of the viscous and inertial resistance parameters is needed to simulate a reliable cross-flow.

This study compares numerical results obtained on a complete muffler geometry (Panigrahi and Munjal, 2007), using the complete geometry and simplified models based on porous baffle interface and porous region to model perforated elements. The simplified model accuracies come from comparing the results obtained with the complete geometry model, establishing whether it is convenient to use the simplified models in the muffler design process. For this purpose, the pressure drop between inlet and outlet is as the principal reference parameter. Moreover, the computational costs in CPU (central processor unit) time and number of cells are evaluated and compared.

2. Muffler geometry

The presented study uses as reference a straight-through perforated tube muffler (Figure 1) with an *OAR* (open area ratio) equal to 1 (Panigrahi and Munjal, 2007). The following equation defines *OAR*:

$$OAR = \frac{4L\varepsilon}{d} \tag{1}$$

where L is the length, d is the diameter of the perforated pipe and ε is the porosity.

The straight-through perforated tube muffler geometry used is reported in Panigrahi and Munjal (2007): the inner pipe, outlined in green, ends with a plug, while the outer one, depicted in grey, has an open end that represents the outlet of the muffler as the flow goes along the y-axis. The perforated pipe, represented in blue, has a porosity of 7%, holes diameter of 3.0 mm and a thickness of 1.5 mm. Table 1 reports the main dimensions of the muffler.

3. Numerical implementation

This section presents the settings used in the numerical simulations, starting from the resistance parameters needed to model with the porous baffle/region the dissipation caused by the flow passing through the holes of the perforated element. Then, the focus is on the

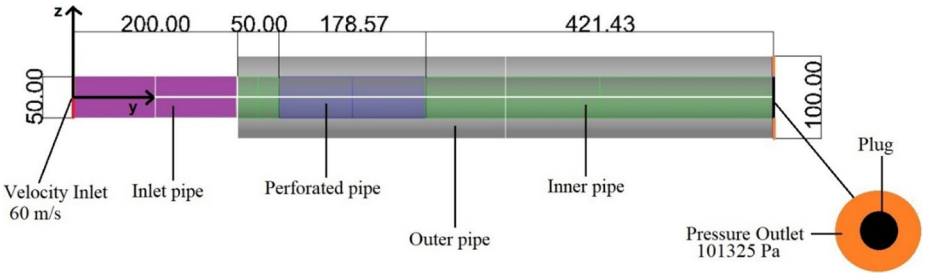

Figure 1.
Straight-through perforated tube muffler geometry

solution method and the boundary conditions adopted for the simulations. Finally, the last part describes the grid independence study performed with the complete geometry model and the simplified ones to select the mesh size.

3.1. Resistance parameters

The viscous and inertial resistance parameters used for the porous baffle interface and the porous region are evaluated based on the Darcy-Forchheimer law. This relation, reported in the following equation, is used to characterize the flow through porous media (Kizilaslan *et al.*, 2018; Tanner *et al.*, 2019):

$$\frac{\Delta P}{L} = -\left(\nu\alpha + \frac{1}{2}V\beta\right)V \tag{2}$$

where L is the length of the porous media, ν is the kinematic viscosity, V is the fluid velocity, α and β are the viscous and inertial resistance coefficients, respectively. The following expressions, proposed by Ergun (Berg, 2013), describe α and β depending on porous media properties such as porosity ε and particle size d_p:

$$\alpha = \frac{150}{d_p^2}\frac{(1-\varepsilon)^2}{\varepsilon^3} \tag{3}$$

$$\beta = \frac{1.75}{d_p}\frac{(1-\varepsilon)}{\varepsilon^3} \tag{4}$$

These expressions are valid for cellular media, made of small spherical particles. Nevertheless, a cellular media constituted by solid filaments connected to form pores is a suitable approximation for a perforated pipe, using the following equivalent particle diameter d_e (Innocentini *et al.*, 1999) in equations (3) and (4):

$$\mathrm{d_e} = 1.5\,\frac{(1-\varepsilon)}{\varepsilon}\,\mathrm{d_c} \tag{5}$$

where d_c is the hydraulic diameter.

In this work, the only resistance parameter considered is the inertial one; the mean local Reynolds number inside the muffler is around 30,000, and, consequently, the viscous contribution is negligible. The computed β parameter is equal to 80,422 $\mathrm{m^{-1}}$, obtained with a d_e of 0.059 m. For the porous region, this value is used in the radial direction, while, in the axial direction, the inertial resistance is set with three higher orders of magnitude, as recommended in the Star-CCM+ user manual.

Table 1. Straight-through perforated tube muffler main dimensions

Component	Length [mm]	Diameter [mm]
Inlet pipe	200.00	50.00
Outer pipe	650.00	100.00
Perforated pipe	178.57	50.00

3.2. Solution method and boundary conditions

The numerical resolution of the Reynolds-averaged Navier–Stokes equations has been performed applying STAR-CCM+ software. The numerical simulations refer to the same physical settings and boundary conditions of the literature reference case (Panigrahi and Munjal, 2007), ensuring compliance between the simulations sets.

Therefore, computations have been performed in steady-state, using a segregated flow model. The segregated solver solves the conservation equations of mass and momentum in a sequential manner, basing on a predictor-corrector approach. A semi-implicit method for pressure-linked equations-type algorithm models the pressure-velocity coupling.

The simulations adopt the realizable k-ε turbulence model; it is a two-equation model that solves transport equations for the turbulent kinetic energy and the turbulent dissipation rate to determine the turbulent eddy viscosity.

The considered working medium through all the simulations is air, having an initial temperature of 623°C, a constant density of 0.39 kg m^{-3} and dynamic viscosity of 4.0 e^{-5} kg $(m\ s)^{-1}$. The calculation domain is presented in Figure 1, showing the muffler geometry and relative boundaries. The boundary conditions setup is as follows:

- velocity-inlet with a flow velocity of 60 m s^{-1};
- pressure-outlet with the atmospheric pressure applied at the open end of the outlet pipe (Figure 1); and
- no-slip condition at the wall boundary, i.e. muffler surfaces.

The calculation domain has been discretized with trimmed mesh, selecting the base size through a mesh sensitivity study reported in the next section. The prism layer has been generated with a total thickness of 5.83 mm and 6 prism layers with a stretching factor of 1.5 to obtain a wall $y^+ \leq 1$. A refining area has been set around the perforated pipe, setting a target value of 20% of the base size for the generated cells. The symmetry has not been considered to capture possible flow cross-effects developing at the centre of the muffler.

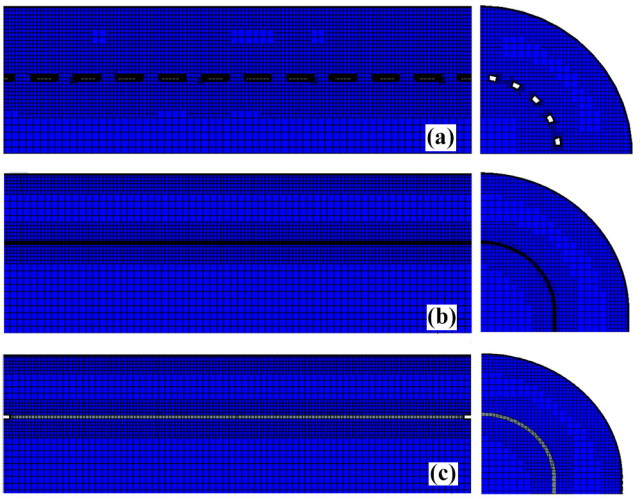

Notes: (a) Complete geometry model; (b) porous baffle interface model; (c) porous region (highlighted in grey) model

Figure 2.
Particular of the mesh along the perforated pipe

Figure 2 reports a mesh detail along the perforated pipe (both longitudinal and transversal plane) for the three models analyzed in this study: the complete geometry model, porous baffle interface model, porous region model.

3.3. Grid independence study

For the mesh sensitivity study, the pressure drop (ΔP) between the inlet and the outlet is the reference parameter and the base size is varied in the range 1.25–20.00 mm with a refinement ratio equal to 2. The grid convergence index (GCI) (Kwaśniewski, 2013) allows identifying whether consecutive mesh refinements have a solution laying or not in an asymptotic region. The index has the following formulation:

$$GCI = 1.25 \left\{ \left(\frac{F_{i+1} - F_i}{F_i} \right) \left[\frac{1}{(r^p - 1)} \right] \right\} \tag{6}$$

where r is the refinement ratio, F_i are the model values obtained with each grid refinement and p is the solution convergence order, expressed in the following equation:

$$p = \ln\left(\frac{F_{i+2} - F_{i+1}}{F_{i+1} - F_i} \right) \Big/ \ln(r) \tag{7}$$

The searching process for the asymptotic solution requires comparing two successive values of *GCI* using the following equation:

$$A_r = r^p \left(\frac{GCI_i}{GCI_{i+1}} \right) \tag{8}$$

When the value of the parameter A_r is near 1, the desired condition is satisfied.

The results of the grid convergence study are summarized in Figures 3 and 4 and Tables 3, 4 and 5. Figure 3 gives a global overview of the ΔP variations among the base size range tested for all three modelling options. Figure 4 reports the convergence curve obtained on the data set with the associated order of convergence p. Both plots represent the pressure drop as a function of the relative step size, which means the actual base size is normalized by the smaller one.

For the complete geometry model (Figure 3), the process reaches convergence decreasing the cell dimensions. An A_r value equal to 1.0 corresponds to base sizes between 2.5 and 5.0 mm (Table 2). Moreover, the convergence order p is around 6.5, which indicates that the high base size meshes are too coarse for the analyses. Accordingly, for the complete geometry model, a mesh base size of 5.0 mm was selected for the computations as it is in the asymptotic range.

Considering the simplified models, a perusal of Figures 3 and 4 shows that the results obtained with the porous region model converge ($p = 1.585$), while the results obtained with the porous baffle interface model have a low convergence order ($p = 0.473$). For the latter case, a mesh base size smaller than 1.25 mm may increase convergence order. However, a test performed with a smaller size still confirms the nature of the results. In any case, a finer mesh increases the computational costs, and the porous baffle interface model may result in no more practical convenience. The low convergence order can be due to the porous interface modelling, as, probably, the Darcy-Forchheimer law is not suitable for proper modelling the

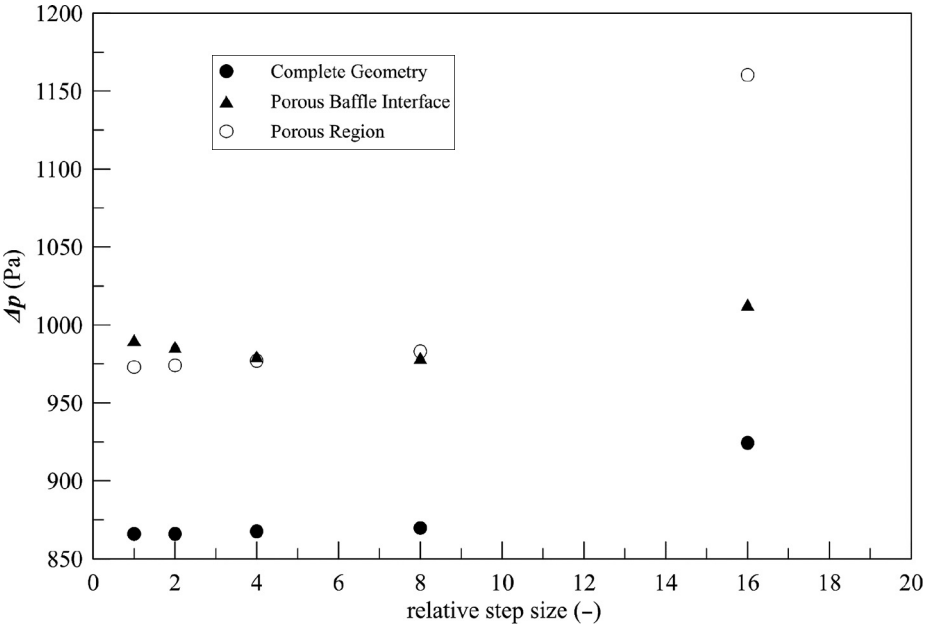

Figure 3.
Pressure drop ΔP for different base sizes

flow through perforated elements. The adoption of experimentally derived resistance coefficients may improve the results. However, such an approach requires a dedicated study in that direction.

Concerning the porous region model, Table 4 summarizes the parameter used to estimate the convergence of the results. The convergence order is here above the linear order, indicating that also higher base size may be appropriate for the study. However, is more appropriate considering also GCI as selection parameter for the base size. As per the complete geometry case, the base size of 5.0 mm grants an A_r value near 1.0 between 2.5 and 5.0 mm. Therefore, regardless of the aforementioned convergence issue, also the porous baffle interface model adopts the same base size as the other simulation sets. Of course, the porous baffle interface simulations will have a higher uncertainty than the other two models, as the simulations will have a higher discretization error.

Comparing the grid independence study performed on both the complete geometry model and the porous region model, the GCI_5 of the complete geometry model is smaller by about 2.5 times in respect to the GCI_5 of the simplified model (Tables 2 and 4). However, the 5 mm base size is in the asymptotic range (Figures 3 and 4) for both models and represents the best compromise between computational costs and accuracy of results. A comparison with the GCI values for the baffle interface is not proficient, as these values are three orders of magnitude higher (Table 3) compared to the other models.

4. Results and discussion

This section firstly compares the results obtained with the complete geometry model with data reported in the literature to evaluate the reliability of the numerical model adopted. Then, the results obtained with the simplified models are analyzed and compared with the complete geometry ones.

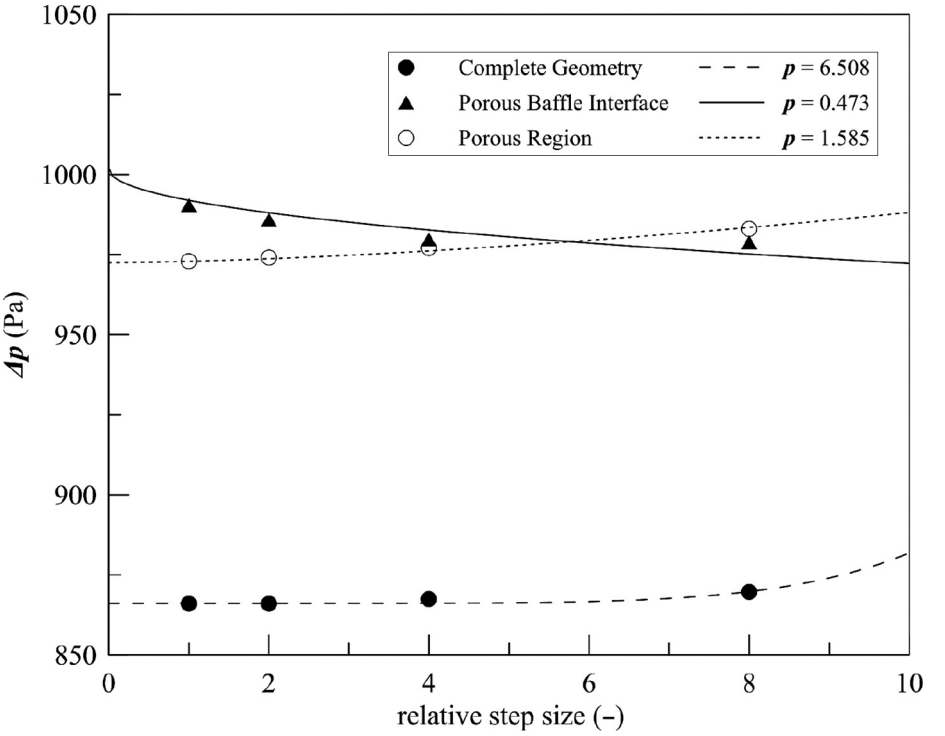

Figure 4.
Convergence order p for the three modelling options

Table 2.
Summary of grids data for the asymptotic solution estimation: complete geometry model

Base size [mm]	GCI	ΔP [Pa]	No. of cells
2.5	$1.44 \cdot 10^{-3}$	866	16,728,484
5.0	$2.88 \cdot 10^{-3}$	868	4,091,228
10.0	0.08	870	900,612

Table 3.
Summary of grids data for the asymptotic solution estimation: porous baffle interface model

Base size [mm]	GCI	ΔP [Pa]	No. of cells
2.5	1.45	986	15,613,684
5.0	2.02	980	3,630,510
10.0	0.29	979	795,636

4.1. Comparison of results with literature data

A comparison between the axial velocity calculated with the complete geometry model and data reported by Panigrahi and Munjal (2007) has been performed to estimate the validity of the numerical model. In Figure 5, it is possible to notice that the velocity trends are in good agreement, although the results obtained in this study show high fluctuations probably due

to the different mesh sizes, especially in the proximity of the perforated pipe. Moreover, Table 5 reports the comparison between velocities in four control points as follows: inlet, the inlet of perforated pipe, the outlet of perforated pipe and outlet. Except for the perforated pipe end, the difference between results is less than 2% and confirms the validity of the numerical model used in this paper. The difference at the outlet of the perforated pipe (peak on the black line) is due to the fluctuations captured with the mesh refinement area set around the perforations to better capture the phenomena generated by the flow through the holes. In conclusion, the adopted modelling for the complete geometry is in line with reference calculations available in the literature. The mean values of the quantity of interest are close, and only the axial velocity in the outer presents significant additional oscillations. However, these fluctuations are in line with the flow observed during the simulations (Figure 6a), as they are representative of the flow coming outside the holes and suggest that, most likely, the data presented in the literature are already a smooth fitting of the axial velocity. In any case, without the availability of experimental data, it is only possible to state the global compliance between the two simulations.

4.2. Comparison between complete geometry and simplified models

Figure 6 shows the velocity fields along the muffler calculated with the complete geometry model and the simplified ones. It is immediate to notice how the porous interface/region (Figure 6b–6c) model does not adequately reproduce the flow through the holes as in the complete geometry (Figure 6a). The flow crosses the porous interface/region through its entire length. The resistance to cross-flow follows the resistance parameters (see *Resistance Parameter* Section).

It is interesting to notice the differences between the flow across the holes among the three different models. The complete geometry gives, reasonably, the best overview of the flow across the muffler. However, the two simplified models present different solutions for the axial velocity. The baffle interface (Figure 6b) detects the flow crossing from inner to outer pipe only in the last part of the interface. The modelling of the porous resistance coefficient can be responsible for this phenomenon, as the porous region model (Figure 6c) allows the crossflow through the entire region length.

Table 4. Summary of grids data for the asymptotic solution estimation: porous region model

Base size [mm]	GCI	ΔP [Pa]	No. of cells
2.5	$3.85 \cdot 10^{-3}$	974	14,998,561
5.0	$7.68 \cdot 10^{-3}$	977	3,484,614
10.0	$2.54 \cdot 10^{-3}$	983	727,944

Table 5. Comparison between modelled velocity (complete geometry model) and data reported in literature (Panigrahi and Munjal, 2007)

Position	Calculated axial velocity [m/s]	Literature axial velocity [m/s]	Difference [%]
Inlet	60.0	60.0	0.0
Inlet perforated pipe	59.0	60.0	−1.7
Outlet perforated pipe	28.0	19.0	+47.0
Outlet	20.0	20.0	0.0

The pressure trend calculated with the three models along the inner and the outer pipe of the muffler is reported in Figure 7: pressure fluctuations are visible only in the complete geometry model, consistently with the velocity fields in Figure 6.

A perusal of Table 6 shows that the ΔP calculated with the porous baffle interface and the porous region models differ from the value obtained with the complete geometry model of about 13% and 12%, respectively. These results are in line with data reported in literature about the use of a simplified model on modelling tubes bundles in heat exchangers (Yang *et al.*, 2014; Prithiviraj and Andrews, 1998). The esteemed pressure drop with the porous model has a deviation of about 10%–20% from both the whole model and experimental data.

In the presented study, the two simplified models predict higher pressure drop values compared to the complete geometry one. Even though the two simplified models have specific uncertainties (due to the convergence order studied in the grid independence study), they are far away from the complete geometry value. The higher uncertainties of both simplified models compared to complete geometry is not sufficient to justify it. Therefore,

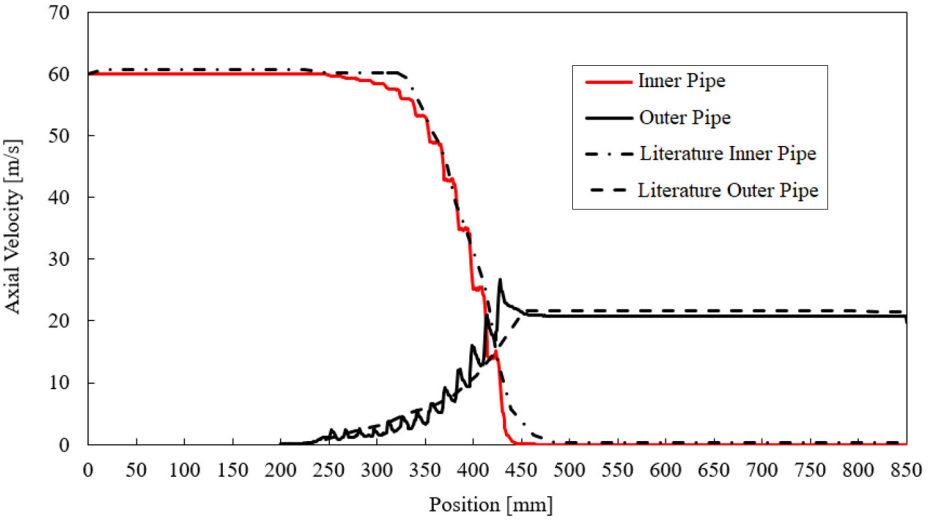

Figure 5.
Comparison between calculated axial velocity (complete geometry model) and literature data (Panigrahi and Munjal, 2007) along the inner and the outer pipe

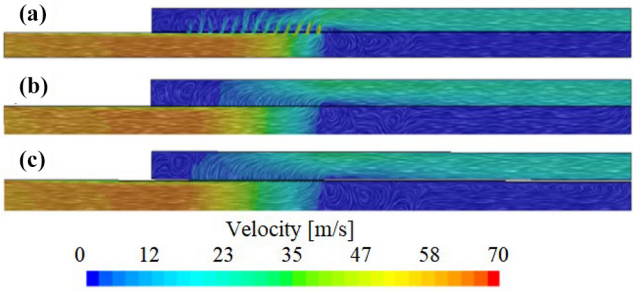

Figure 6.
Velocity field with streamline calculated along the muffler

Notes: (a) Complete geometry model; (b) porous baffle interface model; (c) porous region model

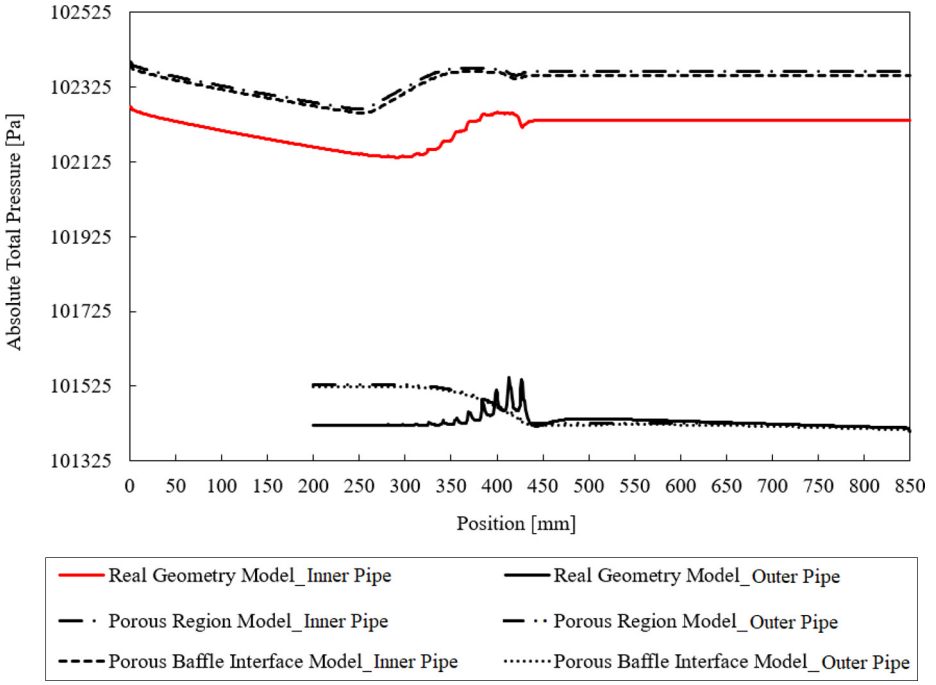

Figure 7.
Absolute total pressure calculated along the muffler inner and outer pipe

Model	No. of cells	CPU time [s]	ΔP [Pa]
Complete geometry	4,091,228	74,533	867
Porous baffle interface	3,630,510 (−11%)	72,850 (−2%)	986 (+14%)
Porous region	3,484,614 (−15%)	64,423 (−14%)	977 (+13%)

Table 6.
Computational costs and ΔP of studied numerical models

being the initial and the boundary conditions and the solver the same between the three models, the reason for the result divergence must be searched in the interface modelling. In conclusion, the analysis of the results allows us to affirm that the inertial resistance parameter, calculated with equation 4, is not adequate to model the interaction between the perforated pipe and the flow.

Table 6 also reports the number of cells and the CPU Time of the three numerical models presented in this paper: the reduction of the number of cells and CPU Time is at most of about 14%–15%. The hardware used for the computations has the following characteristics: one physical processor Intel(R) Core (TM) i7-8565U CPU @ 1.80 GHz 1.99 GHz with four cores and eight logical processors, an installed random access memory of 16.0 GHz and a graphics processing unit NVIDIA GeForce MX250 with 2.0 GB of dedicated memory. According to the reported data, a porous region saves more time than the complete geometry case. A faster calculation increases the attractively of the method once the discrepancy of the results is tolerable for design purposes.

As a final consideration, a porous region model can be even more convenient once the dimension and number of the holes increases. For such cases, modelling issues concerning

the resistance coefficients may be less significant for the final results. Moreover, the complete geometry model will require an even finer mesh to capture the flow through the hole, increasing the calculation time reduction.

5. Conclusions

In this work, the use of both the porous baffle interface and the porous region has been investigated for the perforated elements modelling, using a straight-through muffler available in literature as case study.

Setting the resistance parameters according to the default equation for the porous baffle/region, the ΔP obtained with the numerical simulations is about 13%–14% higher than the value obtained with the complete geometry model, regardless of the simplified model adopted, results that are in line with data reported in literature on heat exchanger modelling. So, the computed inertial resistance parameter is not adequate to properly reproduce the flow through the perforated pipe.

Moreover, for the porous baffle interface model, modelling issues already arise during the grid convergence study. The results highlight that the convergence order was low, pointing to values different from the other models. The divergence of such results suggests dedicating further attention to the baffle interface parameters.

The simplified modelling of the holes does not significantly reduce the computational costs. With the porous baffle interface model, the number of cells is reduced of about 11%. On the other hand, for the porous region model the reduction of cells is around 15%.

However, the use of simplified models allows saving time during the design of the CAD (computer-aided design) model, when possible different values of porosity and hole diameters need to be studied. As an example, a macro allows changing the parameters of the perforated elements without the necessity of re-drawing and re-meshing the model.

It is noticeable that the simplified models do not accurately reproduce the flow through the holes, being the porous pipe crossed by the fluid through the entire interface/region length. This approximation does not allow capturing the local-flow phenomena as pressure and velocity fluctuations or vortices.

According to the presented investigation, only the adoption of the complete geometry model ensures a detailed and accurate analysis of the flow through perforated elements. However, the use of simplified models as porous region and porous baffle interface could be convenient to simplify the CAD modelling and the mesh generation processes during the initial design, obtaining with less effort an estimate of the properties and a comparison between different muffler geometries. The latter option should be tested also for different geometries and holes dimensions to define the range where it is not only convenient but also reliable to use porous region models.

References

Barua, S. and Chatterjee, S. (2019), "CFD Analysis on an Elliptical Chamber Muffler of a C.I. Engine", *International Journal of Heat and Technology*, Vol. 37 No. 2, pp. 613-619.

Berg, A. (2013), Numerical and Experimental Study of the Fluid Flow in Porous Medium in Charging Process of Stratified Thermal Storage Tank, Master of Science Thesis, KTH School of Industrial Engineering and Management Energy Technology, Stockholm.

Chen, Y. and Lv, L. (2015), "Design and evaluation of an Integrated SCR and exhaust Muffler from marine diesels", *Journal of Marine Science and Technology*, Vol. 20 No. 3, pp. 505-519.

Chen, Z., Ji, Z. and Huang, H. (2020), "Acoustic impedance of perforated plates in the presence of fully developed grazing flow", *Journal of Sound and Vibration*, Vol. 485, p. 115547.

Fan, L., Gu, B. and Luo, M. (2020), "A cost-benefit analysis of fuel-switching vs. hybrid scrubber installation: A container route through the Chinese SECA case", *Transport Policy*, Vol. 99, pp. 336-344.

Fu, J., Xu, M., Zheng, W., Zhang, Z. and He, Y., (2021), "Effects of structural parameters on transmission loss of diesel engine muffler and analysis of prominent structural parameters", *Applied Science*, Vol. 173, p. 107686.

Fu, J., Li, J., Chen, W., Zhang, Z., Mao, H. and Tang, Y. (2016), "Performance study of the exhaust purification muffler of a diesel engine", *Multidiscipline Modeling in Materials and Structures*, Vol. 12 No. 4, pp. 635-647.

IMO (2008), "Revised MARPOL Annex VI".

Innocentini, M.D.M., Salvini, V.R., Macedo, A. and Pandolfelli, V.C. (1999), "Prediction of ceramic foams permeability using Ergun's equation", *Materials Research*, Vol. 2 No. 4, pp. 283-289.

Johnsen, K., Kock, F., Strøm, A. and Chryssakis, C. (2019), "Global Sulphur Cap 2020 Update, DNV-GL technical report", available at: www.dnvgl.com/maritime/publications/global-sulphur-cap-2020.html, p. 52.

Jun, F., ZengFeng, Z., Wei, C., Hong, M. and JianXing, L. (2018), "Computational fluid dynamics simulations of the flow field characteristics in a novel exhaust purification muffler of diesel engine", *Journal of Low Frequency Noise, Vibration and Active Control*, Vol. 37 No. 4, pp. 816-833.

Kashikar, A., Suryawanshi, R., Sonone, N., Thorat, R. and Savant, S. (2021), "Development of muffler design and its validation", *Applied Acoustics*, Vol. 180, p. 108132.

Kizilaslan, M.A., Demirel, E. and Aral, M.M. (2018), "Effect of Porous Baffles on the Energy Performance of Contact Tanks in Water Treatment", *Water*, Vol. 10 No. 8, p. 1084.

Kwaśniewski, L. (2013), "Application of grid convergence index in FE computation", *Bulletin of the Polish Academy of Sciences: Technical Sciences*, Vol. 61 No. 1, pp. 123-128.

Li, L., Gang, X., Liu, Y., Zhang, X. and Zhang, F. (2018), "Numerical simulations and experiments on thermal viscous power dissipation of perforated plates", *AIP Advances*, Vol. 8, p. 105221.

Liu, C., Cao, Y., Liu, Y., Zhang, W., Zhang, X. and Ming, P. (2019), "Analysis of Intake Silencer Insertion Loss in a Marine Diesel Engine Turbocharger Based on Computational Fluid Dynamics and Acoustic Finite Element Method", *Journal of Engineering for Gas Turbines and Power*, Vol. 141 No. 9, p. 91012.

Liu, L.Y., Zheng, X., Hao, Z.Y. and Qiu, Y. (2020), "A computational fluid dynamics approach for full characterization of muffler without and with exhaust flow", *Physics of Fluids*, Vol. 32, No 6, p. 66101.

Liu, L.Y., Zheng, X., Hao, Z.Y. and Qiu, Y. (2021), "A time-domain simulation method to predict insertion loss of a dissipative muffler with exhaust flow", *Physics of Fluids*, Vol. 33, No. 6, p. 67114.

Mendez, S. and Eldredge, J.D. (2009), "Acoustic modeling of perforated plates with bias flow for Large-Eddy Simulations", *Journal of Computational Physics*, Vol. 228, pp. 4757-4772.

Mishra, P.C., Kar, S.K. and Mishra, H. (2018), "Effect of perforation on exhaust performance of a turbo pipe type muffler using methanol and gasoline blended fuel: A step to NOx control", *Journal of Cleaner Production*, Vol. 183, pp. 869-879.

Mungodla, S.G., Linganiso, L.Z., Mlambo, S. and Motaung, T. (2019), "Economic and technical feasibility studies: technologies for second generation biofuels", *Journal of Engineering, Design and Technology*, Vol. 17 No. 4, pp. 670-704.

Narasimhan, S.V., Mahesh, S., Sivan, M. and Nair, S.S. (2020), "CFD case studies on the acoustic performance and backpressure changes on modified reactive mufflers", *International Conference on Recent Trends in Mechanical and Materials Engineering, AIP Conference Proceedings 2283, Chennai*, pp. 20005-1:20005-8.

Neshat, N., Hadian, H. and Rahimi Alangi, S. (2019), "Technological learning modelling towards sustainable energy planning", *Journal of Engineering, Design and Technology*, Vol. 18 No. 1, pp. 84-101.

Panigrahi, S.N. and Munjal, M.L. (2007), "Backpressure considerations in designing of cross flow perforated-element reactive silencers", *Noise Control Engineering Journal*, Vol. 55 No. 6, p. 504.

Prithiviraj, M. and Andrews, M.J. (1998): "Three-dimensional numerical simulation of shell and tube heat exchangers. Part II: heat transfer, *Numerical Heat Transfer, Part A: Applications:" An International Journal of Computation and Methodology*, Vol. 33, No. 8, pp. 817-828.

Rao, P.C. and Varma, B.M. (2007), "Muffler Design, Development and Validation Methods", *International Journal of Innovative Research in Science, Engineering and Technology*, Vol. 5 No. 5, p. 14.

Selvakumar, K. and Kim, M.Y. (2016), "A numerical study on the fluid flow and thermal characteristics inside the scrubber with water injection", *Journal of Mechanical Science and Technology*, Vol. 30 No. 2, pp. 915-923.

Shinde, P.V., Desavale, R.G., Patil, V.R., Gawali, P.M. and Patil, S.M. (2020), "Modeling, attenuation and flow field analysis of diesel engine mufer using fluid structure interaction approach and experimental analysis", *SN Applied Science*, Vol. 2, No. 5, p. 920.

Suganeswaran, K., Parameshwaran, D.R., Amirthamani, S. and Palanimohan, D. (2014), "Design and Optimization of Muffler for Manufacturing", *International Journal of Innovative Research in Science, Engineering and Technology*, Vol. 3 No. 4, p. 9.

Swamy, M., Kulkarni, R., Dharmadhikari, R. and Rajput S. (2020), "Estimation of Pressure Drop across Exhaust System by CFD Simulation", *International Research Journal of Engineering and Technology*, Vol. 7, No. 7, p. 7.

Tanner, P., Gorman, J. and Sparrow, E. (2019), "Flow–pressure drop characteristics of perforated plates", *International Journal of Numerical Methods for Heat & Fluid Flow*, Vol. 29 No. 11, pp. 4310-4333.

Thirumurugaveerakumar, S. (2020), "Design and Optimization of Muffler Back Pressure", *International Conference on Physics and Chemistry of Materials in Novel Engineering Applications, AIP Conference Proceedings 2270*, *Chennai*, pp. 120001-1-120001-7.

Venkatagiri, B.R., Raj, S.K., Kasyap, S., Kumar, V.G., Baalamurugan, J. and Alphonse, M. (2020), "Latest Trends in Automotive Muffler – A Review", *3rd International Conference on Frontiers in Automobile and Mechanical Engineering, AIP Conference Proceedings 2311*, *Chennai*, pp. 40019-1:40019-8.

Wang, C.N., Tse, C.C. and Chen, S.C. (2013), "Flow Induced Aerodynamic Noise Analysis of Perforated Tube Mufflers", *Journal of Mechanics*, Vol. 29 No. 2, pp. 225-231.

Yang, J., Ma, L., Bock, J., Jacobi, A.M. and Liu, W. (2014), "A comparison of four numerical modeling approaches for enhanced shell-and-tube heat exchangers with experimental validation", *Applied Thermal Engineering*, Vol. 65, pp. 369-383.

Zhang, H., Fan, W. and Guo, L.-X. (2018), "A CFD Results-Based Approach to Investigating Acoustic Attenuation Performance and Pressure Loss of Car Perforated Tube Silencers", *Applied Sciences*, Vol. 8 No. 4, p. 545.

Corresponding author
Giada Kyaw Oo D'Amore can be contacted at: giada.kyawood'amore@phd.units.it